Composites Science and Technology 69 (2009) 898–904

Contents lists available at ScienceDirect

Composites Science and Technology

journal homepage: www.elsevier.com/locate/compscitech

Effect of carbon nanotubes on the interfacial shear strength of T650 carbon fiber in an epoxy matrix

R.J. Sager [a], P.J. Klein [a], D.C. Lagoudas [a,*], Q. Zhang [b], J. Liu [b], L. Dai [b], J.W. Baur [c]

[a] Texas A&M University, Department of Aerospace Engineering, 3141 TAMU, College Station, TX 77843-3141, USA
[b] University of Dayton, Department of Chemical and Materials Engineering, 300 College Park, Dayton, OH 45469-0240, USA
[c] Air Force Research Laboratory, Materials and Manufacturing Directorate, 1864 4th Street, WPAFB, OH 45433-7131, USA

ARTICLE INFO

Article history:
Received 9 May 2008
Received in revised form 11 December 2008
Accepted 18 December 2008
Available online 23 February 2009

Keywords:
A. Nano composites
A. Carbon fibres
A. Polymer–matrix composites (PMCs)
B. Fibre/matrix bond
B. Fragmentation

ABSTRACT

The interfacial shear strength of carbon nanotube coated carbon fibers in epoxy was studied using the single-fiber composite fragmentation test. The carbon fibers were coated with carbon nanotubes (CNT) on the fiber surface using thermal chemical vapor deposition (CVD). The CVD process was adjusted to produce two CNT morphologies for the study: radially aligned and randomly oriented. The purpose of the CNT coating was to potentially produce a multifunctional structural composite. Results of the single-fiber fragmentation tests indicate an improvement in interfacial shear strength with the addition of a nanotube coating. This improvement can most likely be attributed to an increase in the interphase yield strength as well as an improvement in interfacial adhesion due to the presence of the nanotubes.

1. Introduction

With their small size and exceptional mechanical, electrical and thermal properties, carbon nanotubes (CNT) are unique materials which have come to the forefront of today's materials research. Their exceptional strength, stiffness and failure strain make them attractive reinforcement materials, while their characteristic electrical response to load make them ideal candidates for use as sensors and actuators [1–7]. Their high thermal conductivity provides an opportunity for thermal management applications as well [8,9]. By utilizing one or more of these characteristics along with other materials, truly multifunctional composites could be produced.

Carbon nanotubes are essentially graphene sheets in the shape of a tube whose diameter is on the order of nanometers [10]. Various morphologies exist, including armchair and zigzag, which define the orientation of the lattice with the tube axis (chirality). Other variations such as double walled and multi-walled carbon nanotubes (MWCNT) exist, which are two or more nested SWCNTs. Most carbon nanotubes are produced by one of three techniques: carbon-arc discharge, laser ablation of carbon, or chemical vapor deposition (CVD) [11]. Of these, only chemical vapor deposition provides a method to grow CNTs directly onto carbon fibers, which can then be used in traditional fiber-reinforced polymer composites (FRPC). The CVD process provides direct control of location, alignment, morphology and packing density of CNTs while providing strong bonds with a substrate [12]. For FRPCs, this eliminates problems associated with dispersion and orientation of CNTs within a matrix material. Direct growth of CNTs on reinforcing fibers therefore promises to be a useful method of producing multifunctional nanocomposites where control of dispersion, alignment, length and morphology of CNTs within a composite is desired.

The mechanical behavior of composites depend not only on the properties of the constituent materials, but on the characteristics of the interface(s) between the constituents as well. In continuous fiber-reinforced composites, the load is transferred from the matrix to the fiber through shear. With poor interfacial strength, less shear stress is capable of being transferred to the fiber, creating a weaker, less efficient composite. The interfacial strength can be improved through various methods, the most common being through improving the chemical adhesion of the fiber with the matrix, removing the weak outer layer of the fiber produced during fiber fabrication, or by producing an interphase region through the use of a thin polymer sizing [13,14]. The application of a surface treatment during initial processing is useful in applying a surface chemical group to enhance the interaction of the fiber surface with the matrix while concurrently removing a weak outer surface layer. Drzal et al. [13] showed that the most effective result of applying a surface treatment is the removal of the weak outer layer produced during fiber fabrication. The application of a thin polymer coating, referred to as sizing, is useful in producing an interphase region which has material properties different than the surround-

* Corresponding author. Tel.: +1 979 845 9409; fax: +1 979 845 6051.
E-mail address: lagoudas@aeromail.tamu.edu (D.C. Lagoudas).

0266-3538/$ - see front matter © 2009 Elsevier Ltd. All rights reserved.
doi:10.1016/j.compscitech.2008.12.021

ing bulk matrix. Typically, in epoxy sizings, a higher elastic modulus and lower fracture toughness interphase region is produced by non-stoichiometric chemistry, This results in increasing the shear stress transfer to the fiber while providing an alternative for cracking to proceed into the matrix as opposed to failing the fiber interface [14,15]. While not seen by Drzal et al., the thin polymer sizing may also provide a protective function for the fiber surface during handling.

CNT coated fibers have the potential to increase composite mechanical properties while providing for additional electrical or thermal multifunctionality; however the primary role of fiber-reinforced composites is still structural. As such, it is important to ensure that the structural performance of the composite is maintained or improved along with the improvement in multifunctionality. This study focuses on the effect of CVD applied CNTs on the mechanical properties of carbon fiber-reinforced epoxy composites.

Thostenson et al. [16], have previously demonstrated an improvement in interfacial shear strength of carbon fibers coated with MWCNTs. Thostenson et al. used pitch-based carbon fibers, and assumed that the strength of the fibers would not be affected by the CVD processing; therefore, they did not measure the strength of the fibers after processing. This is a valid assumption, given the stability of pitch-based fibers at their processing temperatures. In this work, PAN-based carbon fibers were used, which were pretreated with an oxygen-containing compound, $MgSO_4$. The PAN-based fibers are not as thermally stable as the more graphitic pitch-based fibers, especially in an environment where oxygen may be present [17]; therefore, the tensile strength of the fibers in this work were measured before and after processing. If a constant fiber strength were assumed, the interfacial strength of the processed fibers could be overestimated using the standard Kelly–Tyson [18] method of calculating interfacial shear strength. Additionally, only one orientation of CNTs, appearing to be randomly oriented, was studied by Thostenson. In this work, with the ability to control the orientation of the CNTs with respect to the fiber axis, an examination into the effect of CNT orientation is possible.

In this study, T650 carbon fibers are coated with multi-walled carbon nanotubes through the use of thermal chemical vapor deposition in both a random and radially aligned morphology. The fiber tensile strength and modulus of CNT coated fibers are then examined using the single-fiber tensile test. These results are then compared to those of untreated sized and unsized T650 carbon fibers in an effort to determine to what degree the fiber mechanical properties are degraded due to thermal CVD growth of CNTs. Additionally, the effect of the presence as well as the orientation of CNTs on the interfacial shear strength of CNT coated carbon fibers is studied using the single-fiber fragmentation test. The interfacial shear strength is calculated using the Kelly–Tyson method.

2. Experimental

A series of single-fiber tensile tests were initially performed on fibers with each type of fiber treatment to determine the effect each treatment had on the axial properties of the fibers. Once the tensile data was compiled, a series of single-fiber fragmentation tests were performed in order to determine the effect of the treatments on the interfacial shear strength between the fiber and the epoxy matrix.

2.1. Materials

The resin used in this study was EPIKOTE 862 resin (Hexion Specialty Chemicals, Inc.) with EPIKURE Curing Agent W (Hexion Specialty Chemicals, Inc.). EPIKOTE 862 is a bisphenol-F epoxy resin with an aromatic amine. Resin was mixed with the curing agent at 100:26.4 by weight. Curing temperature and procedure were 2 h at 121 °C followed by 2 h at 177 °C. EPIKOTE 862/W was used in this test due to its high strain to failure, its transparency, and its ability to adhere well to carbon fiber reinforcement.

The carbon fibers used in this study were Thornel T650 (Cytec Industries), a high modulus polyacrylonitrile (PAN) based fiber used extensively within the aerospace industry with high strength and low strain to failure. It is commercially available in two variants, sized and unsized. The sized fibers are coated with a thin (typically 1 wt.%) epoxy surface coating which is specifically formulated to adhere well with an epoxy matrix, as well as improve handling and decrease damage during processing and handling. The unsized fibers do not have this surface coating. Neither fiber type was subjected to an oxidative surface treatment. Once received, various samples of the unsized fibers were further treated through CVD processing in which MWCNTs were grown on the fiber surface.

2.2. Surface treatments

Two CVD treatments were used; one produced MWCNTs which were radially aligned with respect to the fiber surface, and another which produced randomly oriented MWCNTs with respect to the fiber surface. Growth conditions for the radially aligned MWCNTs included a pretreatment of the fiber surface with $MgSO_4$ in alcohol followed by exposure to Iron Phthalocyanine powder at 900 °C for 15 min in an Ar/H_2 environment. In this configuration, iron is used as the catalyst while the phthalocyanine is used as the carbon source. Growth conditions for the randomly oriented MWCNTs included a pretreatment of the fiber surface with $MgSO_4$ in alcohol followed by exposure to a carbon source of xylene and a catalyst of ferrocene at 800 °C for 30 min in an Ar/H_2 environment. High resolution SEM images were taken of both morphologies to verify orientation and coverage, which can be seen in Fig. 1.

2.3. Single-fiber tensile testing

A series of tests were performed in which a single fiber is subjected to tensile loading in accordance with ASTM D 3379-75. Force and displacement measurements were taken which were then used to determine the ultimate tensile strength and axial modulus of the specimen. Tests were performed on each fiber type in order to determine the effect each surface treatment had on the axial properties. Individual fiber diameters were measured using an optical microscope equipped with a Vickers – A.E.I. Image Splitting Eyepiece. Tensile testing was performed on a Sintech 3365 5 kN material test machine at a rate of 0.05 in/s. Data was collected at a rate of 5 points/s.

2.4. Single-fiber fragmentation testing

The single-fiber fragmentation test (SFFT) has been widely used within the literature to analyze the interfacial shear strength of a fiber embedded within a matrix [13,14,16,19–26]. In this test, a single fiber is embedded axially within a dogbone shaped matrix specimen and subjected to a tensile load. The tensile load is transferred from the matrix to the fiber through shear stress at the interface, causing the fiber to elongate. As the fiber elongates, it begins to fragment, failing at its weakest points. Continued elongation results in continued fragmentation, until all the fragments are too short to transfer enough load to create sufficient tensile stress to break the fiber. By assuming a constant shear stress, the interfacial shear strength can be determined through a simple force balance equation of the fragment:

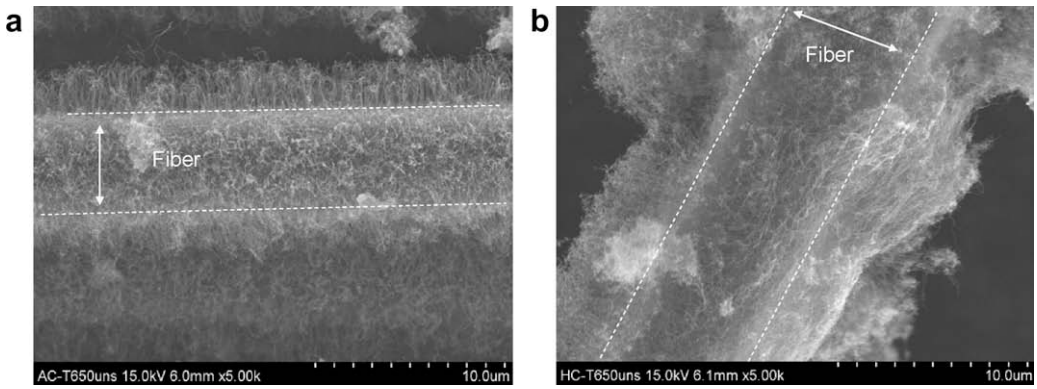

Fig. 1. High resolution SEM images of (a) carbon fiber with radially aligned MWCNTs and (b) carbon fiber with randomly oriented MWCNTs.

$$\tau = \frac{\sigma_f}{2}\left(\frac{d}{l_c}\right) \tag{1}$$

where τ is the interfacial shear strength, σ_f is the ultimate fiber strength at the critical length, d is the fiber diameter, and l_c is the fiber critical length. The assumption of a constant shear stress was originally used by Kelly and Tyson [18] for tungsten and molybdenum wires in a copper matrix. It was assumed that the copper matrix would perform as a rigid-perfectly plastic material, yielding at the interface and producing a constant shear stress along the fiber. In this study, an epoxy thermoset is used, which has a shear yield strength dependent on strain rate. For low strain rates, Gilat et al. [27] showed that Epon 862/W behaves as a ductile material, yielding plastically at stress levels around 50 MPa. Therefore, at low strain rates, the assumption from Eq. (1) of perfectly plastic yielding is valid for the material used in this study.

Because a fiber will fragment whenever its length is greater than the critical length, a range of fragment lengths between l_c and $l_c/2$ will be present upon saturation (Fig. 2). Assuming a normal distribution, the critical length l_c of a fiber can be determined using the measured average fragment length $\bar{l}$ through the equation [26]:

$$l_c = \frac{4}{3}\bar{l} \tag{2}$$

where

$$\bar{l} = \frac{1}{N}\sum_{i=1}^{N} l_i \tag{3}$$

with l_i, the individual fragment lengths and N, the number of fragments within the gauge length. Therefore, when comparing two fibers of equal strength and diameter, the fiber with the shortest critical length will have the highest interfacial shear strength.

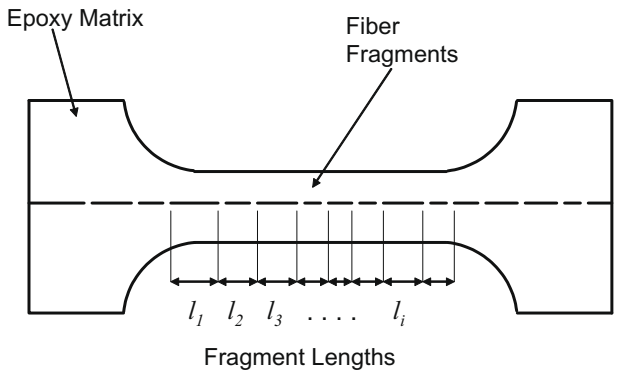

Fig. 2. Schematic of saturated specimen.

The test is performed under a light microscope so that fragmentation could be observed in situ. Polarization is also used to view photoelastic effects such as birefringence caused by debonding of the interface as well as fiber fracture. Under polarization, the epoxy matrix is optically isotropic, but becomes anisotropic when subjected to stress [24]. The presence of bright birefringence at the points of fiber fracture is used here as a method to easily determine the fragment lengths during testing.

2.5. Specimen fabrication

Standard dogbone molds with a 25.4 mm gauge length designed using a metal template. Molds were cast using a silicone rubber compound, GE Silicones RTV664A-1GP, mixed with a curing agent, GE Silicones RTV664B-01P, at a ratio of 10:1. The mold was then degassed for 3 h under vacuum to remove any air bubbles and to ensure a smooth specimen surface. The molds were then allowed to cure at room temperature overnight. Post cure processing at elevated temperatures of 200 °C for 2 h was also performed to ensure that any remaining gasses would evacuate the mold and not disturb the epoxy dogbone specimens during processing.

Once the molds had been prepared, single fibers were placed axially within notches in the molds. Epoxy, which had been prepared and degassed, was then poured into the molds, taking special care to keep the fibers from moving to either side or in the through thickness direction. The specimens were then placed within an oven and cured for 2 h at 121 °C and then for 2 more hours at 177 °C. After the specimens had cooled, they were removed from the molds and prepared for testing. Preparation included sanding down the uneven top of the resin with 600 and 1000 grit sandpaper to an even height of approximately 1.65 mm. The surfaces of the specimens were then polished with 0.5 μm alumina polishing solution until the embedded fiber could clearly be seen and no surface scratches were visible.

2.6. Test procedure

After the specimens have been adequately prepared, they are secured in the test apparatus and subjected to tensile load (Fig. 3a). The entire loading frame is placed under an optical microscope (Nikon Microphot-FXL) equipped with polarizers so that the fragmentation process can be observed insitu (Fig. 3b). Load is applied through the use of a hand screw which pulls a chain upward. This pulling of the chain is translated into a tensile load along the axial direction of the dogbone specimen. A strain gauge is mounted to the test apparatus where the chain meets the specimen holder. The strain gauge is connected to a strain box and was calibrated to display the load applied. Load was

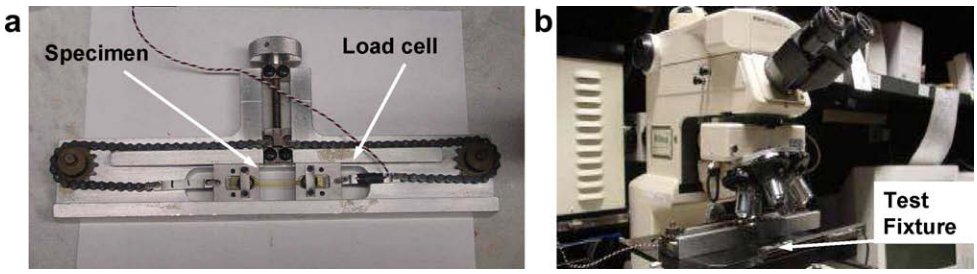

Fig. 3. (a) Fragmentation test fixture. (b) Test fixture under microscope.

originally applied to 267 N and then held for a short time so that fragmentation could be observed. Once the number of fragments was counted, load was then applied in 22 N intervals, stopping with each to observe fragmentation and record images. Fragmentation initiation for all specimens occurred between 311 N and 511 N, with the majority initiating around 378 N. Sized fibers initiated fragmentation at an average of 458 N. Loading of the specimens continued until fragmentation of the fibers ceased or the specimen failed.

Fragmentation of the fiber was observed in situ using polarized light. The use of polarizers allowed for the observance of birefringence within the epoxy matrix. As the fibers break and the interface fails, bright colorful patterns emerged around the fiber–matrix interface. This birefringence effect is a useful tool for observing stress patterns as well as observing the fracture of the opaque carbon fibers. As load is transferred to the fiber, stress will build along the fiber, creating a birefringent effect. When the fiber breaks, the stress drops to zero in the break gap between fiber fragments, producing an area of no birefringence. The observance of birefringent peaks separated by areas of no birefringence can be utilized to denote fiber breaks. Because both the fiber break gaps and the fibers themselves are dark under plain light, breaks within the fiber are difficult to observe. The use of birefringence however, gives the observer a useful tool for easily determining the existence of a fiber break. During testing, fiber fragments were counted using the observance of birefringence gaps while the specimen was under load.

After the number of fragments was counted for each loading increment, load was then applied and the process was repeated. Average fragment length was then determined by dividing the number of fragments at the current load by the gauge length over which the observations were made. Once the fibers ceased to fragment with increasing load, the specimen was said to be saturated and the average fragment length was noted. Some specimens failed before a saturation state was achieved. In these cases, the final fragment length was not considered to be the saturation length and therefore the data was not used in shear strength calculations. The exception to this however, was in the cases of sized fiber specimens. Throughout testing, none of the sized fiber specimens reached a critical length before the epoxy specimen failed. This was due to the increased strain to failure of the sized T650 fibers as compared to the other fibers tested. Because no saturation state was achieved for the sized fibers, the final fragment lengths were taken instead, resulting in an upper bound estimation for the fiber's critical length.

3. Results

3.1. Fiber tensile results

The fiber tensile results, which can be seen in Table 1, clearly demonstrate the effect on which surface treatment plays a role in tensile properties of fibers. Tests revealed a range in ultimate strengths and moduli both within fiber types as well as between fiber types. Sized T650 fibers were measured to have the highest tensile modulus and strength out of all types measured, with modulus and strength values of 217 and 4.02 GPa respectively. As-received unsized T650 fibers demonstrated lower modulus and strength values of 200 and 2.86 GPa, respectively, a decrease of 8% in modulus and 29% in ultimate strength as compared to its sized counterpart. These decreases, especially in ultimate strength, are probably due to damage introduced during the bundling and weaving process as well as during the removal of individual filaments from tows for testing combined with the lack of protection offered by a sizing.

Both nanotube coating processes significantly decreased the tensile strength of the carbon fiber. The ultimate tensile strength of the randomly oriented MWCNT coated fibers decreased 30% from the as-received unsized values to an average value of 1.99 GPa. The tensile modulus decreased by 12.5% to a value of 175 GPa, and the diameter decreased by 11%. The ultimate tensile strength of the aligned MWCNT coated fibers decreased 37% from the as-received unsized values to an average value of 1.79 GPa. The modulus and diameter remained essentially unaffected. As previously stated, the CVD process has been shown to cause degradation of fiber properties through the introduction of surface flaws on the fiber through thermal degradation and surface oxidation. Oxidation can also reduce the diameter of the fiber, which is significant in the randomly oriented MWCNT case due to the 100% longer reaction time compared to the aligned MWCNT case. These effects can be minimized by minimizing the amount of oxygen in the CVD chamber. Subsequent optimization of the growth conditions has resulted in unsized fibers coated with MWCNTs that maintain close to their original mechanical properties [28]. However, these were unavailable at the time of this testing.

It is widely observed that typical reinforcement fibers, including carbon, exhibit a size effect whereby shorter fibers give higher tensile strength measurements. This is due to the presence of flaws in the fiber from the manufacturing process, handling, and environmental effects. Longer fibers will have a greater amount, and likely more severe defects; therefore, the gauge length will affect the measured tensile properties of carbon fibers. A Weibull distribution often emerges as a good representation of fiber strength distribution, and can be used to estimate the length scale effect on tensile properties [29]. Weibull plots for each fiber type were produced using a two-dimensional Weibull statistical method. The Weibull cumulative probability, $\ln(-\ln(1-P))$ for each fiber strength value was plotted versus the logarithm of fiber strength, to produce a linear plot ("Weibull plot"), the slope of which is the Weibull shape parameter, ρ. The cumulative probability of failure, P, for each fiber strength value was estimated by its median rank, m, which in turn was estimated by

Table 1
Measured physical and mechanical properties of single fiber specimens.

Fiber type	Diameter (μm)	Modulus (GPa)	σ_{UTS} (GPa)	ϵ (%)	Weibull shape parameter	No. of samples
Unsized fiber	7.3	200	2.86	1.43	5.21	55
Sized fiber	7.3	217	4.02	1.86	4.32	49
Unsized w/aligned CNT	7.2	182	1.79	0.99	4.02	56
Unsized w/random CNT	6.5	175	1.99	1.13	4.27	62

$$m = \frac{i - 0.3}{n + 0.4} \tag{4}$$

where i is the ascending rank of each strength value, and n is the total number of specimens tested for each fiber type [30]. The Weibull plots can be seen in Fig. 4. For all fiber types tested, few outliers were observed. The resulting shape parameters for each fiber type are shown in Table 1.

3.2. Fragmentation results

Calculation of interfacial shear strength was carried out for each specimen which reached a saturation state using the equations for the shear stress, τ, and the critical length, l_c, as described previously. The average fragment length for each specimen that reached a saturation state was used to calculate that specimen's critical length l_c according to Eq. (2). For each specimen's calculated critical length, the fibers ultimate tensile strength at the critical length was calculated using a simple weakest-link scaling function [29]:

$$\sigma_f = \sigma_{UTS}\left(\frac{l_c}{l_0}\right)^{\frac{-1}{\rho}} \tag{5}$$

where σ_f is the mean fiber tensile strength at the critical length, σ_{UTS} is the measured mean fiber tensile strength from tensile tests, l_c is the fiber critical length, l_0 is the fiber length used in the tensile tests, and ρ is the Weibull shape parameter determined from the tensile test results. The interfacial shear strength τ was then calculated from Eq. (1) using the critical length value and the fiber tensile strength at the critical length. Interfacial strength results for each fiber type can be seen in Table 2.

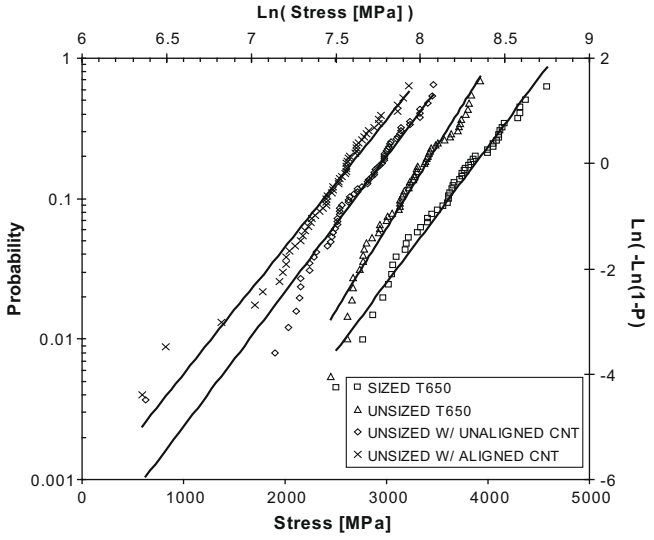

Fig. 4. Weibull plots of tensile treatments. The slopes of the linear curves denote the Weibull shape parameter for that surface treatment.

Tests revealed a large range in critical lengths and thus in calculated interfacial shear strength values as well, especially within the MWCNT coated fiber types. Both of the as-received fiber types performed consistently between their respective specimens in terms of critical lengths. This can be expected due to a consistency in manufacturing processes and therefore a consistency in strength once the major surface flaws were eliminated in the initial few fragmentations. However, it should be noted that within this set of tests, not a single sized fiber specimen achieved a true saturation state before specimen catastrophic failure. This can be seen in Fig. 5 by the lack of a plateau for the sized fiber specimens. For this reason, the average fragment length obtained immediately before specimen failure was used instead. This results in a upper bound for the fiber critical length and thus a lower bound for the interfacial shear strength.

The MWCNT coated fibers demonstrated a larger variation in their critical lengths and thus their calculated interfacial strength values. This variation suggests a non-uniformity of surface qualities among the fibers tested. One explanation of this is a discontinuous or inconsistent deposition of MWCNTs along fibers within the same bundle. Because the CVD process was performed on bundles of fibers, it can be expected that variations in coverage will exist between fibers which were positioned near the outer surface of the fiber bundle as opposed to fibers which were positioned near the middle. Although a concerted effort was made to separate the individual fibers from the same area of the bundle, variations in coverage are unavoidable.

Calculations indicate that sized T650 has the strongest interfacial strength. This is probably due both to the excellent adhesion created between the fiber and the matrix as well as the non-stoichiometric interphase produced by the sizing. Drzal et al. [14] demonstrated that the main effect of a sizing is to produce a brittle interphase region surrounding the fiber. The sizing usually contains less than a stoichiometric amount of curing agent, creating a layer having a higher modulus along with lower fracture toughness. The higher modulus increases the shear stress transfer to the fiber, whereas the decreased fracture strength directs the failure away from the interface and into the matrix. The effect of modulus on shear transfer has been validated using finite element modeling [15]. Fig. 6 demonstrates the photoelastic effects of the various fibers. Interfacial debonding was not seen in any of the sized fiber specimens. Large transverse matrix cracking was seen at the fiber break, indicative of the reduced fracture toughness interphase region created by the sizing.

As expected, the unsized fibers demonstrated the least amount of interfacial strength. Photoelastic observations of the unsized fiber near the fiber breaks demonstrate a thin, flat region of birefringence followed by a bulge of birefringence. This birefringent behavior has been observed by others [13,14,19,24,25] as an indication of interfacial debonding. The presence of interfacial debonding can be associated with a low fiber–matrix adhesion, resulting in poor interfacial strength.

Both of the MWCNT coated fibers indicated interfacial shear strength values higher than the unsized fibers, with the randomly oriented MWCNT coated fibers outperforming the aligned MWCNT

Table 2
Fragmentation test results for various fiber types.

Fiber type	σ_{UTS} (GPa)	Shape parameter ρ	σ_f (GPa)	l_c (μm)	$\tau_{KellyTyson}$ (MPa)
Unsized fiber	2.86	5.21	6.19	338	50.5
Sized fiber	4.02	4.32	10.59	<383	>101.6
Unsized w/aligned CNT	1.79	4.02	5.19	362	56.2
Unsized w/random CNT	1.99	4.27	5.98	229	86.6

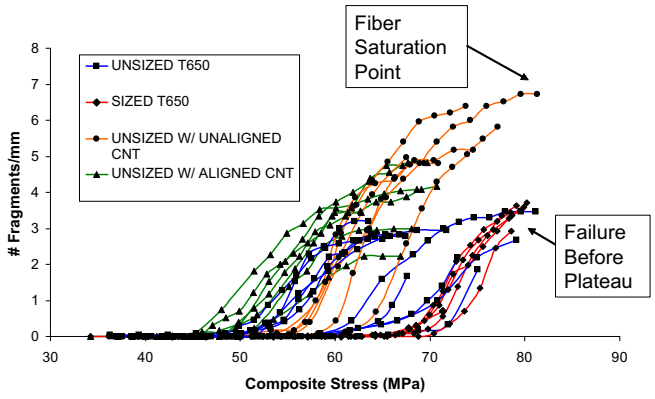

Fig. 5. Plot of number of fragments/mm vs. composite stress for each fiber type tested. The fragment saturation point is determined when the number of fragments remains constant with increasing load. Variations in critical length within individual fiber types can clearly be seen.

coated fibers. Randomly oriented MWCNT and aligned MWCNT coated fibers demonstrated a 71% and 11% increase in calculated shear strength, respectively, over that of the untreated, unsized fiber from which it was processed. This increase is most likely due to the presence of the nanotubes along the interface increasing the adhesion between the fiber and matrix. Observations of the birefringence patterns close to the fiber breaks of the MWCNT coated fibers indicated no interfacial failure and therefore good adhesion. Because the fibers saturated without debonding, it is assumed that the matrix yielded at the interface. The difference in the interfacial strength values between the two MWCNT coatings can therefore be attributed to a difference in the yield strength of their respective interphase regions. Examination of the state of stress in the composite matrix close to the fiber is constructive in explaining the differences in the interphase yield strengths. Close to the fiber, the matrix will be subject to shear stress due to the modulus mismatch with the fiber. Assuming pure shear, the shear stress will result in a principal tensile stress that is at an angle of (±)45° to the fiber axis, and also at an angle of (±)45° to the radially aligned nanotubes. In the case of the randomly oriented MWCNTs, some of the MWCNTs will be aligned with the principal tensile stress direction, resulting in greater load transfer and higher yield strength than the radially aligned MWCNT case.

4. Conclusions

Tensile and single-fiber fragmentation tests were performed on single T650 carbon fibers which had been coated with multi-walled carbon nanotubes through chemical vapor deposition (CVD). Results were compared to commercially sized and unsized fibers in an effort to determine what effect MWCNTs have on the tensile and interfacial properties of a fiber embedded within a polymer matrix. Tensile tests revealed that CVD processing significantly reduces the ultimate tensile strength of the fiber by an average of 37% in the case of the radially aligned MWCNTs and by 30% in the case of randomly oriented MWCNTs. Similarly, a slight reduction in the average tensile modulus of the fiber by 9% and 13% was observed in the radially aligned and randomly oriented MWCNT coated fibers, respectively. Reductions in mechanical properties of the fiber due to processing can be attributed to the addition of surface flaws to the fiber through thermal degradation and surface oxidation. Decreased processing temperatures as well as the elimination of oxygen within the processing chamber have been shown to decrease this degradation in mechanical properties [28].

Single-fiber fragmentation tests were performed on each fiber type in an effort to determine the effect of surface treatment on interfacial shear strength. The Kelly–Tyson model was used to calculate interfacial shear strength from a fiber's critical fragment length and the calculated tensile strength of the fragments. The fragment strength was calculated using a Weibull distribution of fiber strengths calculated using 25.4 mm tensile specimens. Fragmentation results indicated that commercially sized fibers have the highest interfacial shear strength, while unsized fibers had the lowest. Randomly oriented MWCNT and aligned MWCNT coated fibers demonstrated a 71% and 11% increase in interfacial shear strength over untreated, unsized fibers. This increase can be attributed to an increase in both the adhesion of the matrix to the fiber and the interphase shear yield strength due to the presence of the nanotubes. The increase in interphase shear strength observed for the randomly oriented MWCNT case is most likely due to the alignment of MWCNTs with the principal tensile stress direction in the interphase.

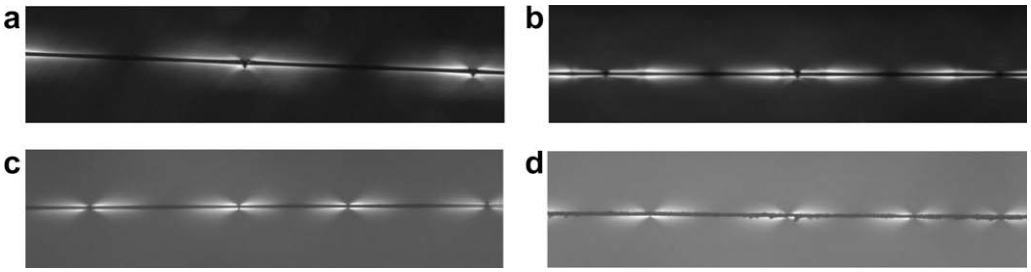

Fig. 6. Birefringence effects of fragmented specimens at 10× magnification. (a) Sized T650. (b) Unsized T650. (c) Aligned CNT. (d) Random CNT.

Acknowledgements

Funding for this research provided by Air Force Research Laboratory, Minority Leaders Program, F33601-05-D-1912.

References

[1] Kong J, Franklin NR, Zhou C, Chapline MG, Peng S, Cho K, et al. Nanotube molecular wires as chemical sensors. Science 2000;287:622–5.
[2] Snow ES, Perkins FK, Houser EJ, Badescu SC, Reinecke TL. Chemical detection with a single-walled carbon nanotube capacitor. Science 2005;307:1942–5.
[3] Peng S, O'Keeffe J, Wei C, Cho K, Kong J, Chen R, et al. Carbon nanotube chemical and mechanical sensors. In: Proceedings of 3rd international workshop on structural health monitoring; 2001. p. 1–8.
[4] Kanga I, Heunga YY, Kimb JH, Leed JW, Gollapudia R, Subra-maniamc S, et al. Introduction to carbon nanotube and nanofiber smart materials. Compos Part B 2006;37:382–94.
[5] Loh KJ, Kim J, Lynch JP, Wong Shi Kam N, Kotov NA. Multifunctional layer-by-layer carbon nanotube-polyelectrolyte thin films for strain and corrosion sensing. Smart Mater Struct 2007;16:429–38.
[6] Thostenson ET, Chou TW. Carbon nanotube networks: sensing of distributed strain and damage for life prediction and self healing. Adv Mater 2006;18:2837–41.
[7] Baughman RH, Cui C, Zakhidov AA, Iqbal Z, Barisci JN, Spinks GM, et al. Carbon nanotube actuators. Science 1999;28:1340–4.
[8] Biercuk MJ, Llaguno MC, Radosavljevic M, Hyun JK, Fischer JE, Johnson AT. Carbon nanotube composites for thermal management. Appl Phys Lett 2002;80:2767–869.
[9] Huang H, Liu C, Wu Y, Fan S. Aligned carbon nanotube composite films for thermal management. Adv Mater 2005;17:1652–6.
[10] Thostenson ET, Li C, Chou TW. Nanocomposites in context. Compos Sci Technol 2005;65:491–516.
[11] Baughman RH, Zakhidov AA, de Heer WA. Carbon nanotubes – the route toward applications. Science 2002;297:787–92.
[12] Dai L, Patil A, Gong X, Guo Z, Liu L, Liu Y, et al. Aligned nanotubes. ChemPhysChem 2003;4:1150–69.
[13] Drzal LT, Rich MT, Lloyd PF. Adhesion of graphite fibers to epoxy matrices: I. The role of fiber surface treatment. J Adhes 1982;16:1–30.
[14] Drzal LT, Rich MT, Koenig MF, Lloyd PF. Adhesion of graphite fibers to epoxy matrices: II. The effect of fiber finish. J Adhes 1983;16:133–52.
[15] Agarwal BD, Bansal RK. Effect of an interfacial layer on the properties of fibrous composites: a theoretical analysis. Fibre Sci Technol 1979;12:149–58.
[16] Thostenson ET, Li WZ, Wang DZ, Ren ZF, Chou TW. Carbon nanotube/carbon fiber hybrid multiscale composites. J Appl Phys 2002;91:6034–7.
[17] Xu Y, Cheng L, Zhang L, Yin H, Yin X, You C. Effects of chemical vapor infiltration atmosphere on the mechanical properties and microstructure of carbon fibers. J Eur Ceram Soc 2001;21:809–16.
[18] Kelly A, Tyson WR. Tensile properties of fibre-reinforced metals: copper/tungsten and copper/molybdenum. J Mech Phys Solids 1965;13:329–50.
[19] Netravali AN, Henstenburg RB, Phoenix SL, Schwartz P. Interfacial shear strength studies using the single-filament-composite test. I: Experiments on graphite fibers in epoxy. Polym Compos 1989;10:226–41.
[20] Skourlis TP, McCullough RL. The effect of temperature on the behavior of the interphase in polymeric composites. Compos Sci Technol 1993;49:363–8.
[21] Nairn JA, Harper SI, Bascom WD. Effects of fiber, matrix, and interphase on carbon fiber composite compression strength. Contractor report 4601. NASA; 1994.
[22] Tripathi D, Jones FR. Single fibre fragmentation test for assessing adhesion in fibre reinforced composites. J Mater Sci 1998;33:1–16.
[23] Zhao FM, Okabe T, Takeda N. Effect of matrix yield properties on fragmentation behavior of single fiber composites. Compos Interf 2002;9:289–308.
[24] Kim BW, Nairn JA. Observations of fiber fracture and interfacial debonding phenomena using the fragmentation test in single fiber composites. J Compos Mater 2002;36:1825–58.
[25] Feih S, Wonsyld K, Minzari D, Westermann P, Lilholt H. Testing procedure for the single fiber fragmentation test. Technical report Risø – R-1483(EN). Risø National Laboratory; 2004.
[26] Ohsawa T, Nakayama A, Miwa M, Hasegawa A. Temperature dependence of critical fiber length for glass fiber-reinforced thermosetting resins. J Appl Polym Sci 1978;22:3203–12.
[27] Gilat A, Goldberg RK, Roberts GD. Strain rate sensitivity of epoxy resin in tensile and shear loading. J Aerospace Eng 2007;20:75–89.
[28] Zhang Q, Liu J, Sager R, Dai L, Baur J. Carbon nanotubes on carbon fibers: influence of growth conditions on fiber tensile properties. In: SAMPE fall technical conference and exhibition, SAMPE, October 29–November 1; 2007.
[29] Beyerlein IJ, Pheonix SL. Statistics for the strength and size effects of microcomposites with four carbon fibers in epoxy resin. Compos Sci Technol 1996;56:75–92.
[30] Johnson LG. The median ranks of sample values in their population with an application to certain fatigue studies. Indust Math 1951;2:1–9.